Received: 29 August 2023 | Revised: 8 October 2023 | Accepted: 17 October 2023 | Published online: 23 October 2023

RESEARCH ARTICLE

Archives of Advanced Engineering Science
2024, Vol. 2(3) 150–159
DOI: 10.47852/bonviewAAES32021602

BON VIEW PUBLISHING

# Comparisons of Static and Dynamic Analyses on Toppling Behaviors of Pile Driving Machinery, etc., on Soft Foundation

**Shouji Toma[1],*, Kenji Seto[1] and Wai Fah Chen[2]**

[1]*Hokkai-Gakuen University, Japan*

[2]*University of Hawaii, USA*

**Abstract:** Toppling accidents of heavy machinery such as pile drivers, cranes, high-altitude work vehicles, and jacks have been recurring in the world. In the past, researches focused to find the overturning moment that causes toppling. However, it is believed that the toppling accidents are related to structural stability issues, in which cases the accidents could possibly occur without any overturning moment. Accidents involving the structural instability are difficult to predict as the directions of load and deformation are different. This unpredictability is considered as a fundamental contributing factor to accidents recurring. Theoretical studies by static and dynamic analyses have been performed by the authors. It was found that not only static deformations but also dynamic inertial forces influence the increased risk of toppling. In the cases of structural instability, dynamic inertial force might amplify angular displacement beyond the critical stability angle, leading to rapid toppling and often resulting in significant disasters. Factors leading to toppling as a trigger include unexpected movement onto weak ground, increased magnitude of load and height, and greater ground incline. Taking those factors into consideration, this paper attempts to elucidate the mechanism of pile drivers' toppling by comparing static and dynamic analyses and providing essential information for preventing accidents. From both static and dynamic analyses, toppling behavior will be described in the load–deformation and the support stiffness–deformation relations. Furthermore, a role of temporal element is illustrated as a quick movement of the machines results in increased risk of toppling.

**Keywords:** pile driver toppling, crane toppling, dynamic analysis of toppling, comparison of static and dynamic analyses, toppling safety, toppling mechanism, overturning of heavy machines

## 1. Introduction

There have been a number of instances on toppling of heavy machinery with high centers of gravity, such as pile drivers, cranes, high-altitude work vehicles, and jacks in Japan [1–4] and other countries [5–7]. In order to prevent recurring such accidents, researches were conducted and reported from different points of view in Japan [8, 9], in the United States [10, 11], in Europe [12], and in India [13]. Mainly, the researches focused on comparing the overturning moment induced by horizontal and/or eccentric vertical forces and the resisting moment induced by the ground support. However, according to the theory of structural stability, the toppling could possibly occur without any overturning moment. From early years, these toppling accidents were attributed to structural stability issues by Toma [14]. Since the toppling accidents of pile driving machines, etc., have been recurring subsequently, researches are reported based on static analysis [15, 16]. Although insufficient support by ground or foundation is a critical cause of these toppling incidents, it is believed that the recurring nature of such toppling accidents is related to the complex and difficult-to-predict structural instability issues. The instability is induced by lack of support force, together with miscellaneous reasons such as increased load, extension of the boom (resulting in higher center of gravity), move onto weak ground, and move onto sloped terrain, among others. In addition, recent research by dynamic analysis has highlighted the role of inertial forces, which results in increasing the risk of toppling [17].

This paper describes static and dynamic analyses of toppling from the perspective of structural stability, comparing and investigating various factors that contribute to the instability of pile drivers. In dynamic analysis, the influence of inertial forces becomes relevant, introducing a temporal element that was not a concern in static analysis. If the duration of instability onset is sufficiently long, static analysis can be applied. In dynamic analysis, the magnitude of inertial forces varies based on the

*Corresponding author: Shouji Toma, Hokkai-Gakuen University, Japan. Email: toma@hgu.jp

**Figure 1**
**Structural models (a) Static analysis and (b) dynamic analysis**

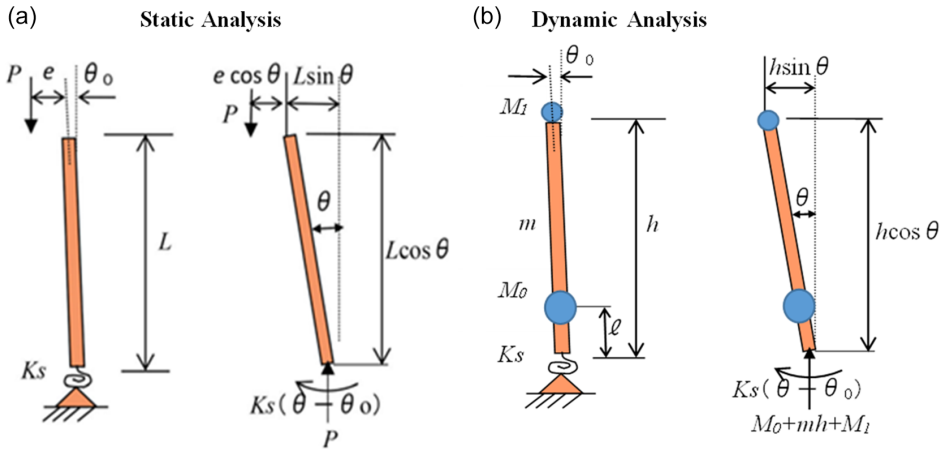


duration time of transition to instability. The inertial force amplifies the magnitude of displacement angles more than in static analysis, implying an increased risk of toppling. By comparing the differences in toppling behavior between static and dynamic analyses, this paper aims to elucidate the mechanism of pile drivers' toppling and provide fundamental information for preventing toppling accidents.

## 2. Structural Models and Governing Equations

### 2.1. Structural models

In this paper, in order to compare and investigate the structural stability issue, the overview of static analysis and dynamic analysis is outlined first. Figure 1 illustrates the structural models for static and dynamic analyses. In Figure 1(a) of static analysis, $P$ represents the total weight of the pile driver (kN), with its application point being the center of gravity $L$ [17]. On the other hand, in Figure 1(b) of dynamic analysis, three masses of the pile driver components are considered: the main body $M_0$, the auger at the top $M_1$, and the boom $m$. Here, $M_0$ and $M_1$ are concentrated masses (kg), while $m$ is a distributed mass (kg/m) with a length $h$ [17]. It should be noted that the units differ between the static and the dynamic analyses. In these figures, the initial inclination $\theta_0$, the rotational spring stiffness $Ks$, and the load eccentricity $e$ are indicated. Additionally, for the case of jack toppling, the structural model simplifies to a single point load at the top, making the structural model depicted in Figure 1(a) applicable to both static and dynamic analyses. Since dynamic analysis of the jack toppling is simpler than the pile driver, it is omitted in this paper.

### 2.2. Equilibrium equations for static analysis

In static analysis, the governing equation expressing the displacement behavior of the pile driver is derived from the equilibrium of forces shown in the structural model of Figure 1(a), as follows [18]:

$$Ks(\theta - \theta_0) - P(L\sin\theta + e\cos\theta) = 0 \tag{1}$$

From the above equation, the load–displacement angle relationship can be obtained as:

$$P/P_{cr} = (\theta - \theta_0)/(\sin\theta + e\cos\theta/L) \tag{2}$$

Here, $P_{cr}$ represents the critical elastic load and is given by:

$$P_{cr} = Ks/L \tag{3}$$

When calculating the load–displacement angle curves for varying initial inclination angles using Equation (2), the result is shown in Figure 2. The curves in Figure 2 were certified by numerical computer analysis [15, 19]. In addition, Figure 3 illustrates the relationship between the rotational spring stiffness $Ks$ and the displacement angle $\theta$ for a pile driver with certain parameters, obtained from Equation (1). From these figures, it is evident that an increase in the initial tilt angle $\theta_0$ leads to larger displacement angles and a higher susceptibility to toppling.

The stability limit $\theta_u$ shown in Figures 2 and 3 is defined as the toppling angle where the restoring force disappears,

**Figure 2**
**Load–displacement angle curves (static analysis)**

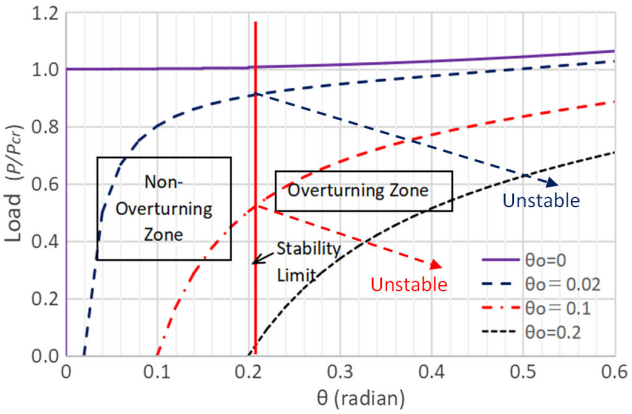

**Figure 3**
**Rotational spring stiffness–displacement angle curves (static analysis)**

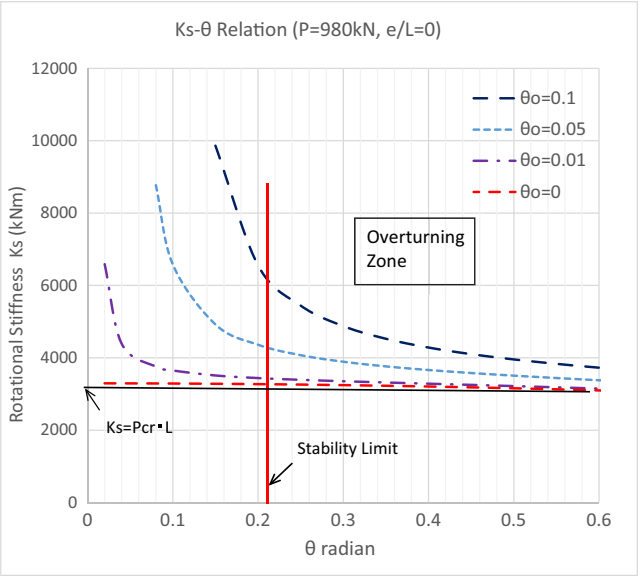


**Figure 4**
**Stability limit angle $\theta_u$**

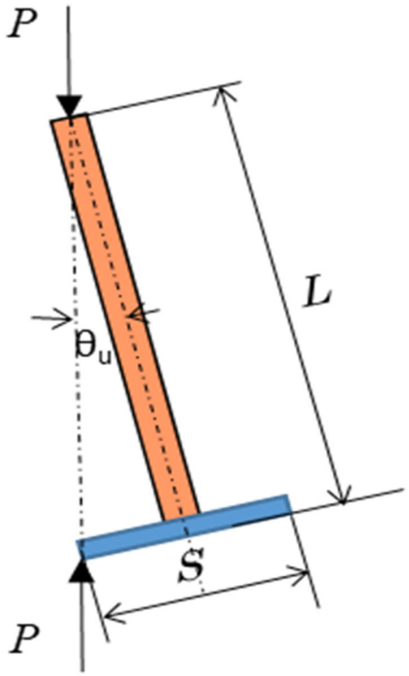


as represented in Figure 4. It is defined by the following equation:

$$\theta_u = \tan^{-1}(S/2L) \tag{4}$$

where $S$ is the track spacing, and $L$ is the height of overall center of gravity.

It should be noted that Equation (4) is determined by the dimensions of the pile driver and is independent of the magnitude of load. When the inclination angle of the pile driver exceeds the toppling angle (stability limit) $\theta_u$, as shown in Figure 2, the load–displacement angle curve slopes downwards, indicating instability.

## 2.3. Equations of motion for dynamic analysis and its solutions

In dynamic analysis, the governing equation describing the displacement behavior of the pile driver is derived from the structural model in Figure 1(b), leading to the following equations of motion [17]:

$$I\frac{\mathrm{d}^2\theta}{\mathrm{d}t^2} + \gamma\frac{d\theta}{dt} - T\,sin\theta + K_s(\theta - \theta_0) = 0 \tag{5}$$

Here, the first term represents inertia moment; the second is damping moment; the third is overturning moment; and the fourth is righting moment. The moment of inertia (second-order moment) $I$ and the first-order moment of the pile driver's weight $T$ are calculated as follows:

$$I = \left(M_1 + \frac{1}{3}mh\right)h^2 + M_0l^2 \tag{6}$$

$$T = \left(M_1 + \frac{1}{2}mh\right)gh + M_0gl \tag{7}$$

where $g$ is the acceleration due to gravity, $\ell$ is the height of gravity center to $M_0$, and $h$ is the boom length (see Figure 1(b)).

The relationship among $L$, $T$, and $P$ is given by $L = T/P$. It is important to note that an increase in the center of gravity height $L$ not only leads to a smaller critical elastic overturning load $P_{cr}$ of Equation (3) in static analysis, resulting in larger displacement angles as shown in Figure 2, but also causes the toppling angle to decrease, making the system more prone to toppling, as per Equation (4). In dynamic analysis, however, the second-order moment of inertia term in Equation (5) increases as the overall center of gravity of the pile driver or crane rises, contributing to the increased susceptibility to toppling.

Solving Equation (5) with damping force set to zero (damping coefficient $\gamma = 0$), the following displacement response equation is obtained [17]:

$$\theta(t) = \frac{\omega_0}{\omega}\sin(\omega t) + (\theta_0 - \theta_c)\cos(\omega t) + \theta_c \tag{8}$$

For the case of initial velocity $\omega_0 = 0$, the equation simplifies to:

$$\theta(t) = (\theta_0 - \theta_c)\cos(\omega t) + \theta_c \tag{9}$$

in which the angular frequency of vibration $\omega$ and the central angle $\theta_c$ are expressed as follows:

$$\omega = \sqrt{\frac{K_s - T}{I}},\ \theta_C = \frac{\theta_0}{1-\alpha}(> \theta_0) \tag{10}$$

in which, the parameter $\alpha = T/Ks = P/P_{cr}$.

Equation (9) represents the free oscillation with the center of oscillation at $\theta_c$ and the single amplitude $(\theta_0 - \theta_c)$. In this context, hereinafter dynamic analysis is conducted without considering damping forces. Now, by using Equation (9) and considering the initial condition of initial inclination angle $\theta$ $(t = 0) = \theta_0$, an example of the displacement angle-time curves can be plotted as shown in Figure 5 [17]. In this example, it is found that the pile driver will overturn at approximately $t = 3.8$ s with the

**Figure 5**
**Displacement angle-time curves**

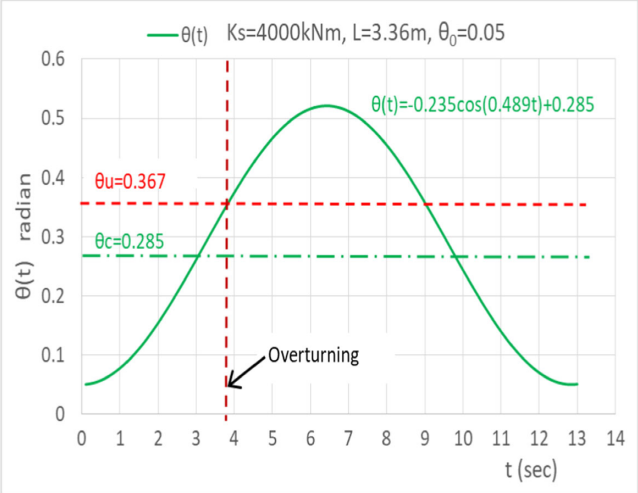


overturning angle (stability limit) $\theta_u = 0.367$ rad., just after the displacement angle exceeds the center of the oscillation $\theta_c$.

Next, when we derive expressions for the displacement angular velocity and the acceleration from Equation (9), they become as follows:

$$\frac{d\theta}{dt} = (\theta c - \theta o)\omega \sin \omega t \tag{11}$$

$$\frac{d^2\theta}{dt^2} = (\theta c - \theta o)\omega^2 \cos \omega t \tag{12}$$

When plotting the inclination angular velocity and acceleration from the above equations for the case of Figure 5, they are shown in Figure 6. In this case, as evident from Figures 5 and 6, the inclination angular velocity starts from zero at the initial condition ($t = 0$), reaches its maximum when the displacement angle is at the center of oscillation at around $t = 3.2$ s, and returns to zero at the maximum displacement angle at around $t = 6.4$ s. In this example, it can be found that when the overturning occurs at around $t = 3.8$ s, the inclination angle velocity is still significant while in static analysis the inclination stops at the center of oscillation, i.e., around $t = 3.2$ s, before reaching the overturning angle (stability limit) $\theta_u$. The relationship between displacement inclination angle, angular velocity, and acceleration becomes clear when examining the tangent

**Figure 6**
**Displacement angle velocity and acceleration curves**

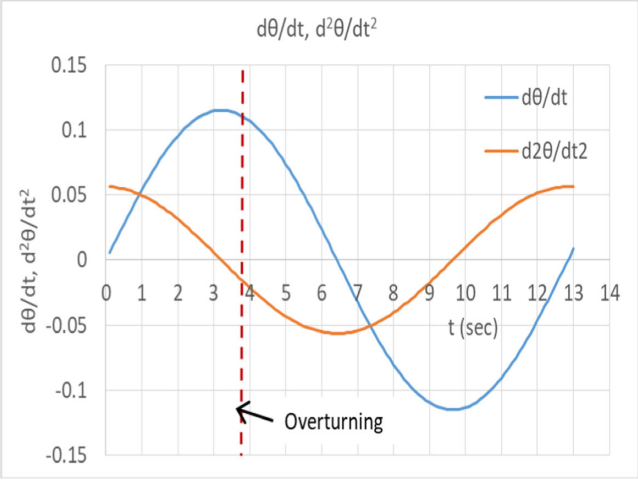


angles of the curves shown in Figures 5 and 6, as they are related through differentiation and integration.

## 2.4. Behaviors of displacement angle in dynamic analysis

Next, when using Equation (9) with the initial condition set as an initial inclination angle $\theta(t = 0) = \theta_0$, the load–oscillation center angle curve can be obtained as shown in Figure 7 [17]. This figure looks the same as Figure 2 in static analysis, but the horizontal axis in Figure 7 represents the displacement angle with respect to the center of oscillation $\theta_c$ while it is merely the displacement angle in static analysis. The figure illustrates example of total amplitude ($\theta_{max} - \theta_{min}$) or single amplitude ($\theta_c - \theta_0$) centered at $\theta_c$. In dynamic analysis, the center of oscillation is the point where the angular velocity is at its maximum, this differs totally from static analysis, where it corresponds to the equilibrium stopping point. Additionally, when comparing initial inclination angles $\theta_0 = 0.05$ and 0.1, it is evident that larger initial inclination results in larger amplitude.

**Figure 7**
**Load–displacement angle curves (dynamic analysis)**

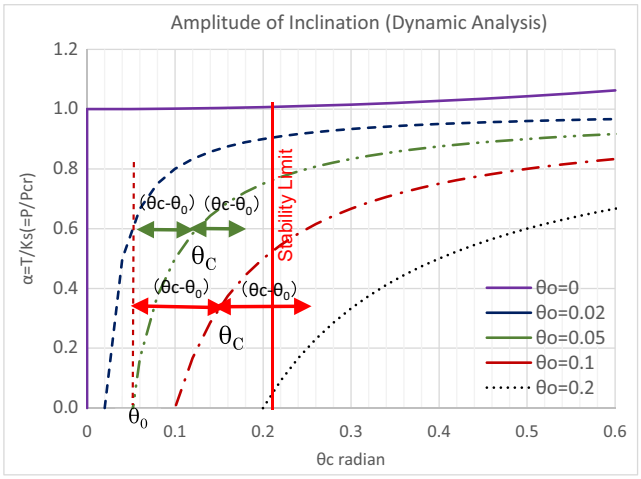


For a pile driver with certain parameters, the rotational spring stiffness–displacement angle curves from dynamic analysis results are shown in Figure 8 [17]. In this figure, a comparison of amplitudes is shown for initial inclination angles $\theta_0 = 0.05$ and 0.01. Similar to Figure 7, it can be observed that larger initial inclination angles result in larger amplitudes. As stated before, the free oscillation shown in Figures 7 and 8 assumes zero damping, and when damping force is considered, the oscillation amplitudes become smaller. In cases of high damping, there is a possibility that the system returns to equilibrium without oscillating (overdamping). However, in general, for heavy machinery like pile drivers that undergo slow inclined oscillations, it is expected that damping forces are relatively small.

In past accidents, it was reported that attempts were made to reposition the inclined pile driver in a direction to reduce the tipping moment, but these attempts eventually led to toppling incidents [20]. A possible reason for this outcome is that the inertial moment was larger than the reduction in the tipping moment. In such cases, once the heavy machinery starts to tilt due to factors like hidden insufficient support, it becomes difficult to restore it to its original position. Hence, cautious consideration must be taken when dealing with weak ground conditions. Furthermore, in scenarios where the load is increased rapidly, as

**Figure 8**
**Rotational spring stiffness–displacement angle curves**

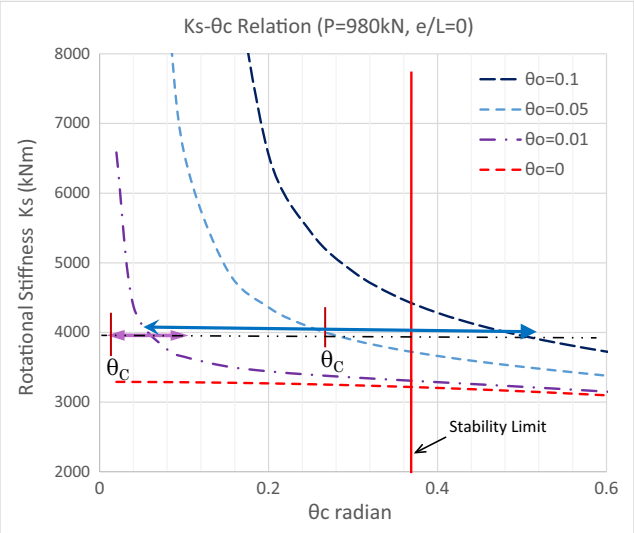


with cranes or jacks, there is a risk of toppling due to the influence of inertial forces once tilting begins. In the next, the discussion will explore the temporal changes in these dynamics.

## 3. Toppling Behaviors in Load–Displacement Angle Relationship

### 3.1. Behaviors in instantaneous movement

Toppling of pile drivers and similar machines often occurs when there is an imbalance, such as increased load during operation, elevated load height, or movement onto weak ground. These factors can all be considered as direct triggers for overturning of pile drivers. As a result, it can be inferred that increasing the value of $\alpha = P/P_{cr}$ leads to structural instability, which is a fundamental factor in toppling. Explaining this state through static analysis, as shown in Figure 9 the equilibrium point A moves directly above to the imbalanced point B' if assumed this transition occurs instantaneously (in a very short time). Then, when transitioning back towards the equilibrium direction C', if the overturning inclination angle (stability limit) $\theta_u$ is exceeded, the machinery will tip over. This toppling mechanism is referred to as "the equilibrium transition type" [17].

A similar movement can be explained using dynamic analysis in Figure 10 [17]: starting with the state of B' as the initial condition, free oscillation represented by Equation (9) begins. Unlike the scenario in Figure 9, the motion does not come to a halt at equilibrium point C'; rather, due to the influence of inertial force, the displacement angle further increases until reaching D'. Thus, dynamic analysis reveals that in this way the risk of toppling increases significantly.

**Figure 9**
**Toppling behavior in instantaneous move (static analysis)**

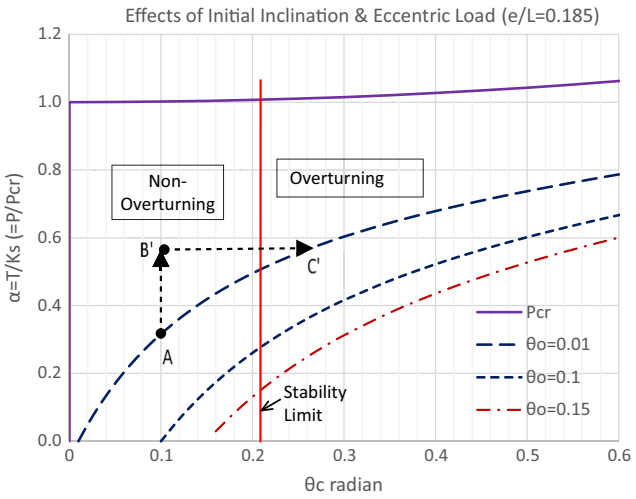


**Figure 10**
**Toppling behavior in instantaneous move (dynamic analysis)**

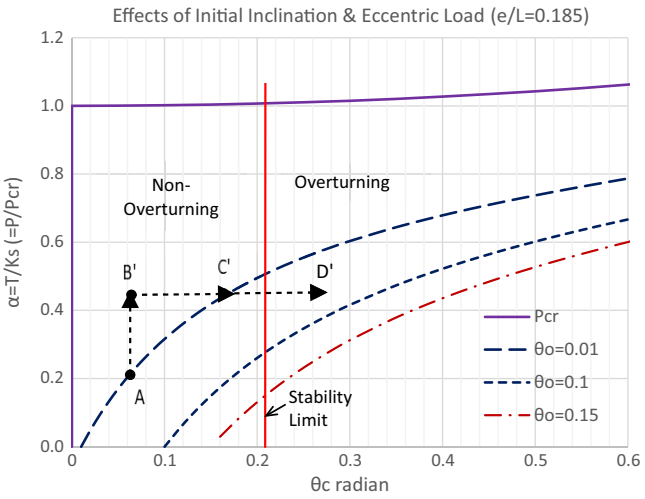


### 3.2. Behaviors in gradual movement

In the previous section, the transition from balanced state A to imbalanced state B' was assumed to occur instantaneously (in a very short time). However, if this transition happens slowly enough, the displacement angle would gradually move along the equilibrium curve in a static manner. Real changes in displacement angles are likely to occur over a certain period of time, placing them between instantaneous and gradual transitions. In other words, as shown in Figure 11, the change from A to B' involves a certain

**Figure 11**
**Toppling behavior in gradual move (static analysis)**

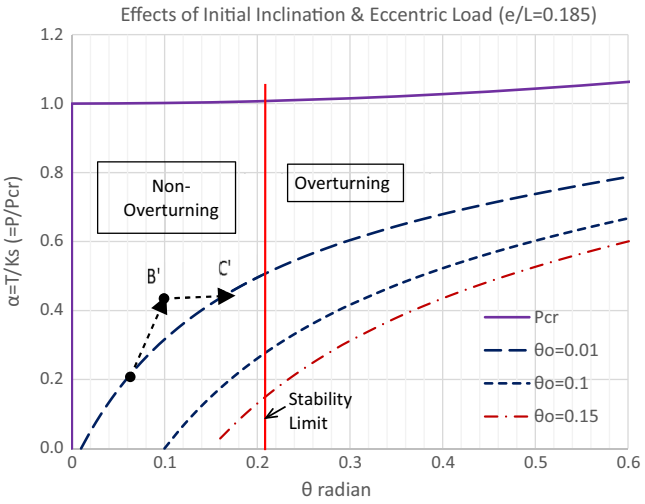

increase in displacement angle and moves in an upward diagonal direction. Then, it is considered to move from the momentarily paused imbalanced point B' to the equilibrium point C' and stops, as envisioned in static analysis.

In dynamic analysis, when using B' as the initial condition, the phenomenon becomes oscillatory, and as seen in the previous section, the displacement angle increases up to the return point D' beyond the equilibrium point C' (the center of oscillation). This behavior is illustrated in Figure 12, and comparing it to the case of instantaneous movement (Figure 10), it is evident that the position of the maximum inclination angle D' is smaller. In other words, dynamic analysis reveals that when moving instantaneously (in a very short time), the amplitude becomes larger, and the maximum inclination angle also increases compared to when moving slowly. For instance, when the load is increased quickly, this sudden change is more likely to lead to instability.

**Figure 12**
**Toppling behavior in gradual move (dynamic analysis)**

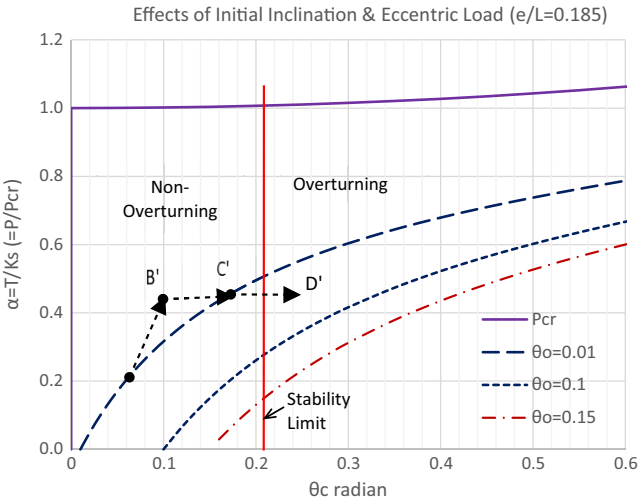


## 4. Toppling Behaviors in Rotational Stiffness–Displacement Angle Relationship

### 4.1. Behaviors in instantaneous movement

In the context of the load–displacement angle relationship, the behavior when moving onto a weak ground was discussed in the previous section. Now, we examine the case of a pile driver with certain parameters moving onto a weak ground in the context of the rotational spring stiffness–displacement angle relationship. Moving onto weak ground implies a reduction in rotational spring stiffness. If this reduction occurs instantaneously, then, as shown in Figure 13, the transition from the balanced point A to the point B or B' directly below will take place. In static analysis illustrated in Figure 13, when attempting to return from these imbalanced points to the balanced point C or C', the system becomes unstable if it surpasses the stability limit angle [17].

On the other hand, as depicted in Figure 14 in dynamic analysis, the phenomenon becomes oscillatory when using B or B' as initial conditions [17]. Due to the inertial forces, the displacement angle may increase beyond the balanced point C or C', making it more prone to toppling over. According to these behaviors of displacement, it can be found that the shaded regions in

**Figure 13**
**Instantaneous move onto soft ground (static analysis)**

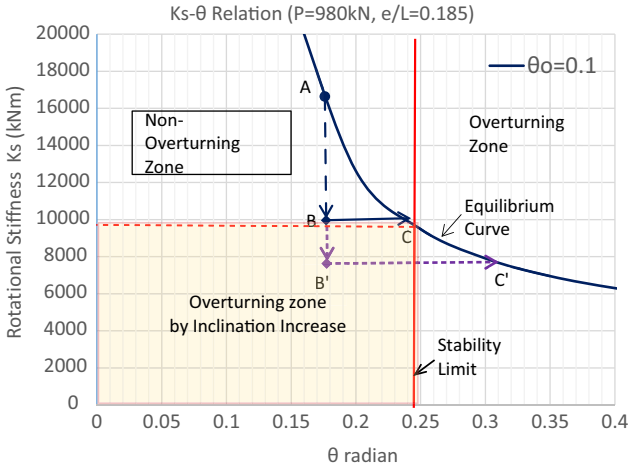


Figures 13 and 14 indicate the range of instability. In the case of static analysis shown in Figure 13, the required rotational stiffness is the intersection between the equilibrium curve and the stability limit. On the other hand, in the case of dynamic analysis in Figure 14, it is determined such that the maximum displacement angle reaches the stability limit, or as to have the same amplitudes on both sides centered at the equilibrium curve. It is obvious that dynamic analysis has a wider range compared to static analysis.

**Figure 14**
**Instantaneous move onto soft ground (dynamic analysis)**

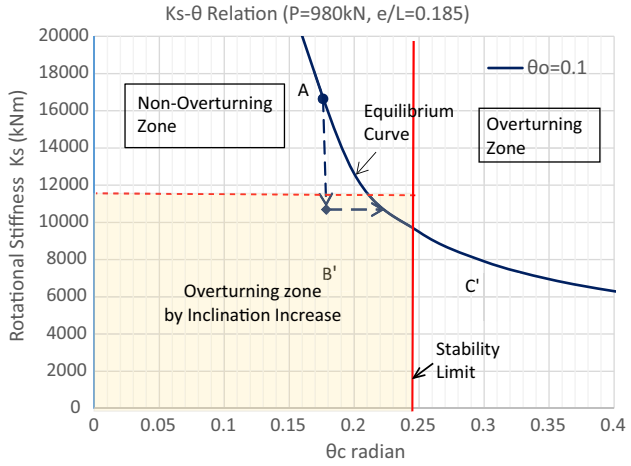


### 4.2. Behaviors in gradual movement

When a pile driver with certain parameters gradually moves onto a weaker ground, as the displacement angle during the movement process gradually increases, it is presumed that the displacement will also increase diagonally downward, similar to the previous section, as depicted in Figures 15 (static analysis) and 16 (dynamic analysis). In static analysis, the displacement comes to a halt along the equilibrium curve, whereas in dynamic analysis, it continues to increase further, making the system more prone to toppling over. As can be seen in Figures 14 and 16 of dynamic analysis, the intersection of the maximum displacement

**Figure 15**
**Gradual move onto soft ground (static analysis)**

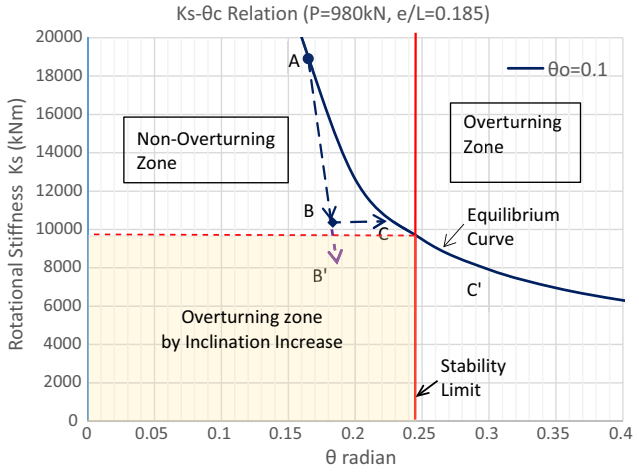


**Figure 16**
**Gradual move onto soft ground (dynamic analysis)**

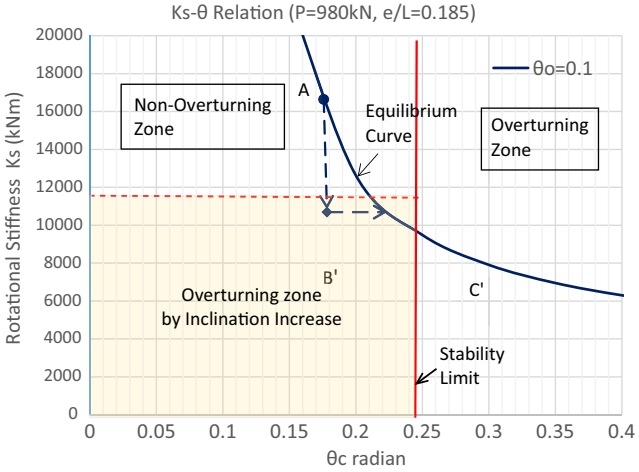


angle and the stability limit indicates the required rotational stiffness, which is the upper line of the shaded area.

## 5. Cases of Increasing Initial Slope Angle

### 5.1. Instantaneous increase of initial slope

Here, we consider the case where a pile driver moves onto sloped terrain. Let us consider a case as shown in Figure 17, where the pile driver, starting from point A with an initial tilt angle $\theta_0 = 0.02$, instantaneously moves to point B at 0.05. In static analysis, since inertial forces are not considered the displacement stops at equilibrium point B. However, in dynamic analysis, as depicted in Figure 18, the displacement angle increases up to point C, which has the same amount of displacement as between points A and B (neglecting damping). During this interval, if the pile driver exceeds its overturning stability angle (stability limit), it will topple over.

**Figure 17**
**Instantaneous increase in initial slope (static analysis)**

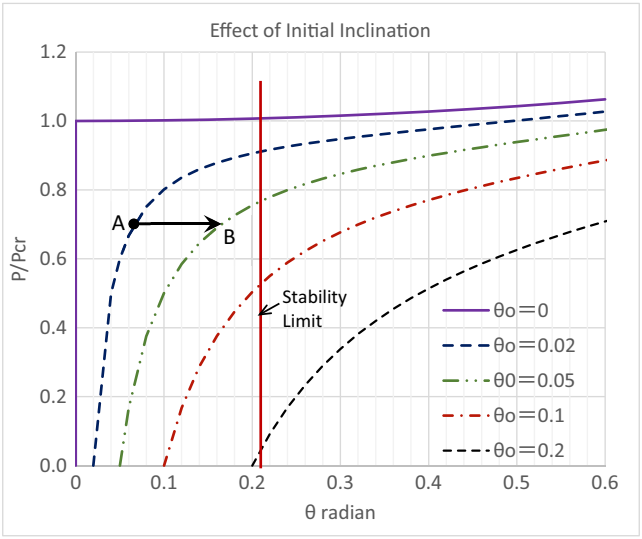


**Figure 18**
**Instantaneous increase in initial slope (dynamic analysis)**

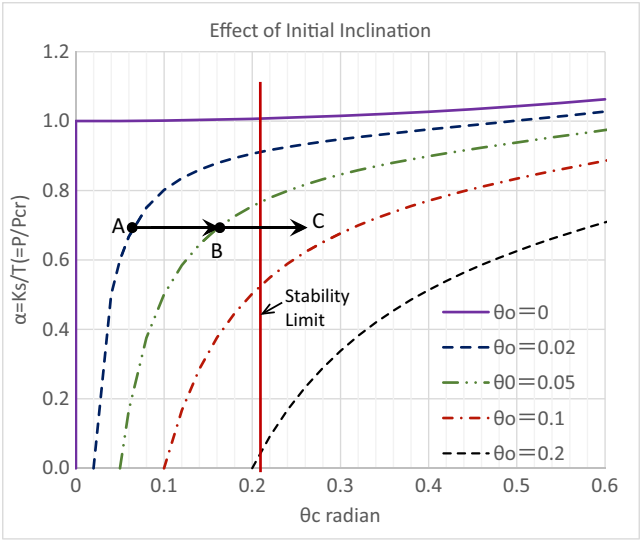


### 5.2. Gradual increase of initial slope

Next, considering the scenario where the movement onto the sloped terrain is taken place gradually, in static analysis, similar to the instantaneous movement case shown in Figure 17, the equilibrium point B on $\theta_0 = 0.05$ is reached and also stopped there as shown in Figure 19. On the other hand, in dynamic analysis, it is anticipated to exhibit an intermediate behavior between Figures 17 and 18. In other words, as shown in Figure 20, the displacement between points B and C would be smaller than the displacement between points A and B. The magnitude of displacement between B and C becomes larger with higher moving velocity. Consequently, according to dynamic analysis, the speed of movement onto the sloped terrain affects the degree of toppling risk, with a greater increase of the risk as the slope becomes steeper at a faster rate. Naturally, with

**Figure 19**
**Gradual increase in initial slope angle (static analysis)**

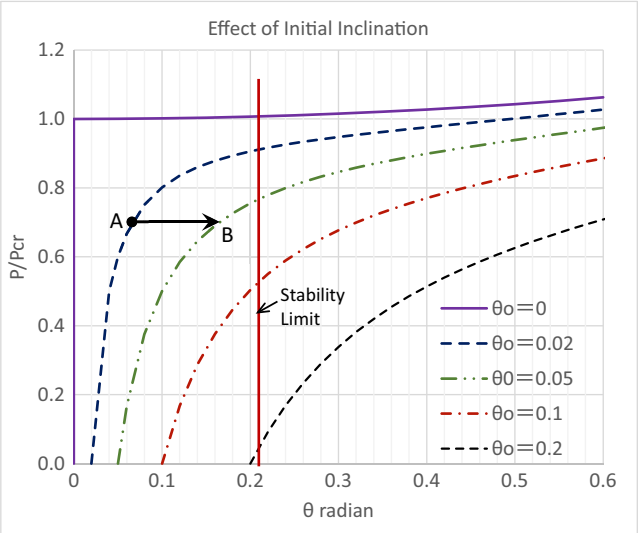


**Figure 20**
**Gradual increase in initial slope angle (dynamic analysis)**

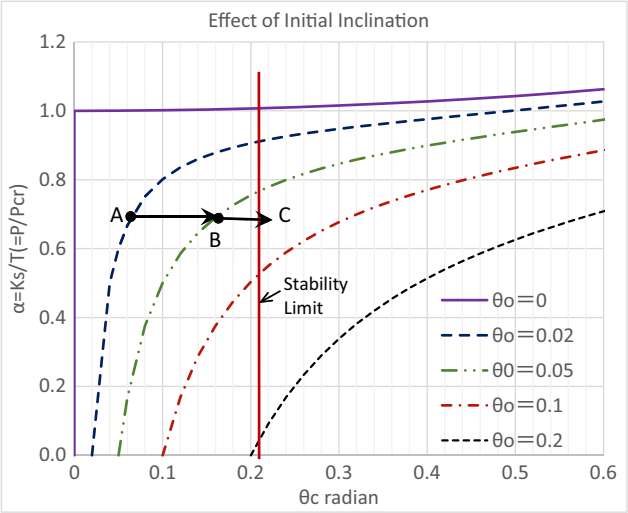


greater differences in slope, the movement from A to B to C becomes larger, making toppling more likely.

## 6. Evaluation for Toppling Safety

In this section, the evaluation of safety considering dynamic analysis is discussed. To maintain toppling safety, the maximum inclination angle must not exceed the toppling inclination angle (stability limit), as shown in the inequity:

$$\theta_{max} < \theta_u \tag{13}$$

The maximum inclination angle is obtained from Equation (9) as follows [17]:

$$\theta_{max} = 2\theta_c - \theta_0 = (1+\alpha)\theta_c \tag{14}$$

By substituting Equations (14) and (4) into Equation (13), the toppling safety evaluation equation becomes as follows:

$$(1+\alpha)\theta_c < tan^{-1}\left(\frac{S}{2L}\right) \tag{15}$$

When plotting the maximum inclination angle from Equation (14), it becomes as shown in Figure 21, which must not exceed the toppling inclination angle (stability limit). The critical load at that moment is indicated by the red dashed line in Figure 21. The ratio of $\theta_u$ to $\theta_{max}$ is defined as the safety factor $\zeta$, which can be used as an evaluation criterion to ensure safety:

$$\zeta = \theta_u/\theta_{max} > S_f \tag{16}$$

**Figure 21**
**Maximum inclination angle ($\omega_0 = 0$)**

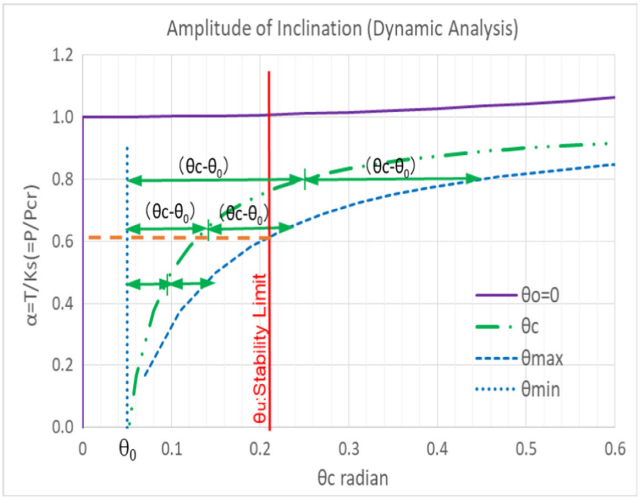


As a suggestion for the safety factor, it might be recommended to use $S_f = 1.2$ to 1.5, depending on the site conditions. The maximum inclination angle $\theta_{max}$ in Equation (14) is based on the assumptions that movement is instantaneous and damping forces are ignored. Considering that the oscillation amplitude is maximized by these assumptions, if a smaller value like 1.2 is adopted for $S_f$, then the critical load value (red dashed line) in Figure 21 would decrease by a factor of 1.2. Additionally, Figure 21 illustrates three different oscillation amplitudes for the case of an initial inclination angle $\theta_0 = 0.05$. It is also evident that as the load increases, the oscillation amplitude becomes larger.

## 7. Case of Initial Angular Velocity $\omega_0 \neq 0$

In dynamic analysis conducted so far, an assumption was made that the initial angular velocity $\omega_0$ is zero. However, in scenario where sudden gusts of wind occur or prestressed force is released, it is plausible to have a non-zero initial inclination angular velocity, i.e., $\omega_0 \neq 0$. In these cases, the maximum inclination angle can be expressed by the following equation [17]:

$$\theta_{\max} = \sqrt{(\theta_0 - \theta_c)^2 + (\omega_0/\omega)^2} + \theta_c \tag{17}$$

From the above equation, it can be observed that the oscillation amplitude relative to the oscillation center $\theta c$ increases due to the presence of $\omega_0$. An example of this behavior is illustrated in Figure 22. Naturally, when compared to the case without initial inclination angular velocity as shown in Figure 21, the oscillation amplitude increases and the critical load value (indicated by the red dashed line) decreases. Consequently, the risk of toppling becomes greater.

**Figure 22**
**Maximum inclination angle ($\omega_0 \neq 0$)**

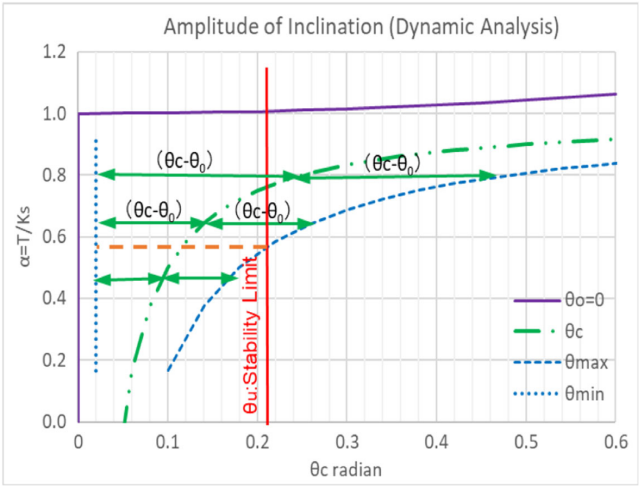


## 8. Evaluation of Rotational Stiffness

Throughout the previous discussions, it has become evident that the rotational spring stiffness *Ks* plays a significant role both in the equilibrium equations for static analysis and the equations of motion for dynamic analysis. While these governing equations assume linearity for *Ks*, the actual behavior is likely more complex. A more precise approach would involve conducting computer-aided structural analysis with a nonlinear consideration, particularly from a geotechnical engineering perspective.

The evaluation of rotational spring stiffness can be theoretically assessed, but in this context, let us consider an approach based on field measurements. As depicted in Figure 23, the rotational spring stiffness can be determined by measuring the inclination angle $\theta$ and the toppling moment. From the definition, the rotational spring stiffness *Ks* can be expressed using the following formula:

$$Ks = PL \sin\theta/\theta \tag{18}$$

During these measurements, it is crucial to ensure that they are performed within an angle range that sufficiently guarantees safety against toppling. By determining the rotational spring stiffness through practical measurements, the assurance of safety can be more robust. This method is effective for conducting the model tests to verify the analytical results presented in this paper.

**Figure 23**
**Measurement of rotational spring stiffness**

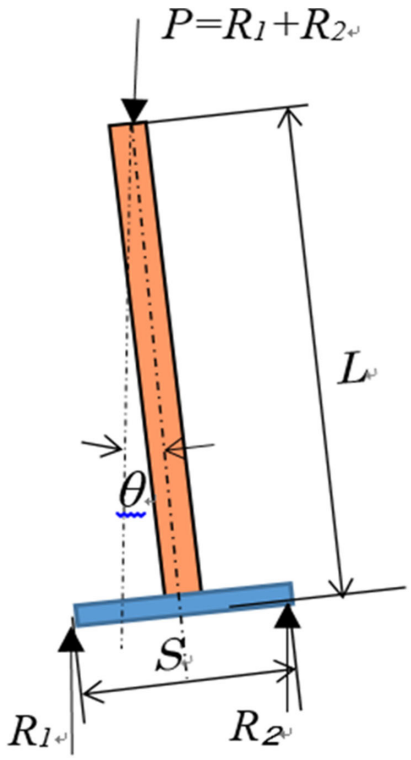


## 9. Conclusions

Heavy machinery with a high center of gravity, represented by pile drivers and cranes, is prone to toppling accidents. So far, researches have been conducted by the authors to elucidate the toppling mechanism from the perspective of structural instability. In this context, it has been shown that the initial incline angle has a significant impact, and recent dynamic analyses have indicated that they are more prone to toppling due to dynamic inertial forces. Based on these research findings, this paper further examined the toppling mechanism by comparing static analysis and dynamic analysis.

The results revealed that rapid increases in the magnitude and height of the load led to a greater inertial force and a larger displacement inclination angle, thereby escalating the risk of toppling within a short period. For instance, when a pile driver moves onto weak ground or when the load on a crane increases, the shorter the duration of these changes, the greater the inertial forces become, making them more prone to tipping. Furthermore, since inertial forces involve a second-order moment, the influence of height of gravity center becomes more pronounced in dynamic analysis compared to static analysis. By examining the toppling behavior of machinery like pile drivers from both static and dynamic perspectives, the toppling process has become clearer.

In order to verify the theoretical work given in this paper, numerical computer analysis and/or experimental research are expected in the future. Also, the theoretical results such as load–displacement curves in static analysis and the inertial force in dynamic analysis should be examined by using actual data taken from the toppling accidents in the past. Furthermore, since theory of structural stability used in this paper is limited within elastic analysis, the future investigation should contain nonlinearity of the materials, especially for ground strength. Nevertheless, it is

believed that the elastic analysis provides valuable information for the toppling mechanism and can serve for making safer precautions against toppling accidents, which have been recurring in the world.

## Postscript

It is worth noting that although not directly addressed here, incidents involving the fall of bridge girders during construction are also recurring. The authors believe that the fundamental cause lies in the instability of portal frame structures leading to the toppling of jacks. The underlying mechanism is fundamentally the same as that of pile driver, making the findings presented in this paper applicable. If a bridge girder supported by jacks were to tip over during their operation, the dynamic effects driven by inertial forces, as addressed here, might be influencing the outcome. Structures with large loads and high centers of gravity, like the jacks supporting bridge girders, require careful consideration for structural stability, similar to pile drivers.

## Ethical Statement

This study does not contain any studies with human or animal subjects performed by any of the authors.

## Conflicts of Interest

The authors declare that they have no conflicts of interest to this work.

## Data Availability Statement

The data that supports the findings of this study is openly available with toma@hgu.jp, and would be shared upon request via email.

## References

[1] Japan Crane Association (2024). Ground stability measures for mobile cranes at work sites. Retrieved from: https://cranenet.or.jp/susume/susume00_09.html (in Japanese).

[2] Japan Construction Machinery and Construction Association. (2017). *Crane related accidents-examples of disaster*. Retrieved from: https://jcmanet.or.jp/bukai-iinkai/kensetsugyou-bukai/saigai-jirei/ (In Japanese)

[3] Nikkei Business Publications. (2000). Accidents under construction, preventing measures for recurrence by learning from great 70 accidents, overturning accidents of heavy machines. *Nikkei Construction*, *Special Issue*, 186–189 (in Japanese).

[4] Nikkei Business Publications. (2016). Accident case (1) fall of erection girders, lost balance due to leaning jacks. *Nikkei Construction*, *649*, 40–43 (in Japanese).

[5] Eskişar, T., & Akboğa Kale, Ö. (2022). Evaluation of pile driving accidents in geotechnical engineering. *International Journal of Occupational Safety and Ergonomics*, *28*(1), 625–634.

[6] HSB. (2014). *Piling rigs overturning on construction sites: A guide to loss prevention*. Retrieved from: https://www.munichre.com/hsbeil/en/insights/guides-to-loss-prevention1/construction-guides-to-loss-prevention/hsbei-1294-piling-rigs-overturning-on-construction-sites-rgn.html

[7] Pile Driving Contractors Association. (2017). *Pile driving safety and environmental best management practices*. Retrieved from: https://www.piledrivers.org/files/b523f7da-eb1f-4110-ac6a-bf8a8b93886b–c79aca8b-018d-437f-a7e5-081fdeedbaa8/9-2017-pdca-safety-and-environmental-best-management-practices.pdf

[8] Hori, T., Tamate, S., & Suemasa, N. (2010). Measurement of shakes and ground contact pressure of a drill rig by the self-propelled experiments. *JSCE Journal of Geotechnical and Geoenvironmental Engineering*, *66*(2), 342–355.

[9] Kunishima, K., & Toyoda, K. (1991). Tachikawa City, the falling accident of the pile driver. Retrieved from: https://www.shippai.org/fkd/en/cfen/CD1000142.html

[10] Pile Driving Contractors Association. (2019). *Working platforms*. Retrieved from: https://www.piledrivers.org/blog/working-platforms

[11] Pile Driving Contractors Association. (2021). *Working platforms recommended industry practices*. Retrieved from: https://www.piledrivers.org/publications/working-platforms-recommended-industry-practices/

[12] Anderson, K. (2021). *How to calculate the necessary support under a crane*. Retrieved from: https://www.internationalcranes.media/news/how-to-calculate-the-necessary-support-under-a-crane/8012492.article

[13] Pai, B. A., Prajwal, J. T., Srijan, S., & Bharath, M. N. (2019). Prevention of toppling of heavy vehicles using gyroscopes. *International Journal of Research in Engineering, Science and Management*, *2*(5), 234–236.

[14] Toma, S. (2002). A study on the causes of toppling accidents of mobile cranes and similar machinery. In *Proceedings of the Hokkaido Branch of the Japan Society of Civil Engineers*, *58*, 62–65 (in Japanese).

[15] Toma, S., & Chen, W. F. (2023). Some aspects of overturning mechanisms of pile driving machine on soft foundation. *American Journal of Civil Engineering*, *10*(6), 225–232.

[16] Toma, S., & Chen, W. F. (2023). Overturning mechanisms of jacks, cranes and pile driving machines. *Structural Engineering International*, *33*(3), 399–407. https://doi.org/10.1080/10168664.2022.2074339

[17] Toma, S., Seto, K., & Chen, W. F. (2023). Dynamic analysis for overturning of pile driving machine, etc., on soft ground. *Transactions on Engineering and Computer Sciences*, *11*(2), 61–81.

[18] Chen, W. F., & Lui, E. M. (1987). *Structural stability: Theory and implementation*. USA: Prentice Hall.

[19] ARK Information Systems. (2023). *International cranes and specialized transport*. Retrieved from: https://www.ark-info-sys.co.jp/jp/product (In Japanese)

[20] Tamate, S., & Hori, T. (2009). Factors influencing support conditions at construction site for toppling of pile driving machines. In *Proceedings of the Symposium on Construction Methods and Construction Machinery* (in Japanese).

**How to Cite:** Toma, S., Seto, K., & Chen, W. F. (2024). Comparisons of Static and Dynamic Analyses on Toppling Behaviors of Pile Driving Machinery, etc., on Soft Foundation. *Archives of Advanced Engineering Science*, *2*(3), 150–159. https://doi.org/10.47852/bonviewAAES32021602